BULLETIN OF THE CHEMICAL SOCIETY OF JAPAN, VOL. 45, 1281—1288(1972)

Magnetic Circular Dichroism Studies on High-intensity Bands of d^8 Square-planar Metal Halides

Hajime KATÔ

Department of Chemistry, Faculty of Science, Kobe University, Kobe

(Received July 6, 1971)

The magnetic circular dichroism (MCD) of certain d^8 square-planar metal halides is studied theoretically on the basis of the molecular orbital theory. The ground state wavefunctions of $PtCl_4^{2-}$ and $PdCl_4^{2-}$ are calculated by the semi-empirical ASMO SCF MO method for valence electron systems. The line shape of the MCD of the allowed transition is investigated in detail; the calculated line shape is in good agreement with the observed line shape. The results strongly suggest that the transitions at 43400 cm^{-1} and 46200 cm^{-1} in $PtCl_4^{2-}$ are $^1A_{1g}\rightarrow{}^1A_{2u}(b_{2u}—3b_{1g}$ and $3a_{1g}—2a_{2u})$ and $^1A_{1g}\rightarrow{}^1E_u(5d—6p)$ respectively, and that the transition at 44900 cm^{-1} in $PdCl_4^{2-}$ is $^1A_{1g}\rightarrow{}^1E_u(1)$.

The electronic spectra of the d^8 square-planar metal halide complexes have been studied by many investigators,[1] and the spectrum has been assigned variously depending on the choice of the ordering of the orbital energy.[2-5] Interest has been focused on the absorption spectrum of $PtCl_4^{2-}$, the assignment of which has many different possibilities. The weak absorption spectrum of a single crystal of K_2PtCl_4 below 36000 cm^{-1} was observed with light polarized parallel to and normal to the symmetry axis of the $PtCl_4^{2-}$ ion.[3] The results of these observations have narrowed the assignment possibilities considerably. However, the polarized spectrum for the high-intensity band has not been reported because of the experimental difficulties.

The MCD spectra below 36000 cm^{-1} for a solution of K_2PtCl_4 in dilute HCl were first reported by Martin, Foss, and their coworkers.[6] The MCD spectra of $PtCl_4^{2-}$, $PdCl_4^{2-}$, $PdBr_4^{2-}$, $AuCl_4^-$, $AuBr_4^-$, and $Pd(NH_3)_4^{2+}$ in solution and K_2PtCl_4 crystal at 4°K

1) a) A. J. Cohen and N. Davidson, *J. Amer. Chem. Soc.*, **73**, 1955 (1951); b) A. J. Cohen and R. A. Plane, *J. Phys. Chem.*, **61**, 1096 (1957); c) G. H. Ayres and B. L. Tuffly, *Anal. Chem.*, **24**, 949 (1952); d) J. Chatt, G. A. Gamlen, and L. E. Orgel, *J. Chem. Soc.*, **1958**, 486, e) *Ibid.*, **1959**, 1047; f) J. G. Fraser, F. E. Beamish, and W. A. E. McBryde, *Anal. Chem.*, **26**, 495 (1954); g) S. Kida, This Bulletin **33**, 587 (1960); h) A. K. Gangopadhayay and A. Chakvavorthy, *J. Chem. Phys.*, **35**, 2206 (1961); i) C. K. Jφgensen, *Advan. Chem. Phys.*, **5**, 119 (1963).

2) R. F. Fenske, D. S. Martin, Jr., and K. Ruedenberg, *Inorg. Chem.*, **1**, 441 (1962); J. R. Miller, *J. Chem. Soc.*, **1965**, 713.

3) a) D. S. Martin, Jr., M. A. Tucker, and A. J. Kassman, *Inorg. Chem.*, **5**, 1298 (1966); *Ibid.*, **4**, 1682 (1965); b) D. S. Martin, Jr., and C. A. Lenhardt, *Ibid.*, **3**, 1368 (1964); c) H. B. Gray and C. J. Ballhausen, *J. Amer. Chem. Soc.*, **85**, 260 (1963); d) P. Day, A. F. Orchard, A. J. Thomson, and R. J. P. Williams, *J. Chem. Phys.*, **42**, 1973 (1965).

4) H. Basch and H. B. Gray, *Inorg. Chem.*, **6**, 365 (1967).

5) F. A. Cotton and C. B. Harris, *ibid.*, **6**, 369 (1967).

6) D. S. Martin, Jr., J. G. Foss, M. E. McCarrvulle, M. A. Tucker, and A. J. Kassman, *Inorg. Chem.*, **5**, 491 (1966).

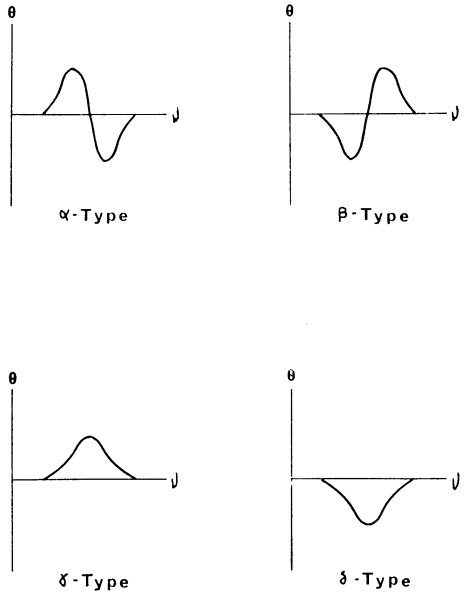

Fig. 1. The characteristic behavior of MCD in the vicinity of wave number corresponding to electronic absorption bands.

over the visible-UV spectral region were reported by McCaffery, Schatz, and Stephens.[7] The MCD curve exhibits its most striking characteristics in the vicinity of wavelengths corresponding to the electronic absorption bands. Some characteristic curves are shown in Fig. 1; we shall call them α-type, β-type, γ-type, and δ-type curves. The main features of the MCD curve around the absorption bands have been outlined previously,[8-10] and it has been shown that the MCD changes sign (α- or β-type) at the absorption maximum only when the excited state or the ground state is degenerate. However, the information which can be obtained from the difference between the α-type and β-type curves has not yet been used sufficiently. Further efforts in these areas are important, and considerable studies are expected.

In this paper, theoretical studies will be carried out on the MCD of the high-intensity bands of d^8 square-planar metal halides from the viewpoint of the MO theory. The line-shape of the MCD is studied in detail, and the observed bands are assigned on the basis of the line-shape analysis. As we will show later, this assignment does not depend strongly on the ordering of the calculated orbital energies. We give a quantitative discussion of the MCD intensity in $PtCl_4^{2-}$ and $PdCl_4^{2-}$, and it is then extended to the interpretation of the high-intensity bands in $PdBr_4^{2-}$, $AuCl_4^-$, and $AuBr_4^-$.

Calculations

A. Theory and MO Formulation. The quantum mechanical theory of MCD was developed around 1930,[11-14] and recently the quantitative expressions for the dispersion have been reported.[9,15,16] The contributions of the $a\rightarrow j$ transition to the MCD of molecules under a longitudinal magnetic field, H_s, along the z-axis are expressed as molar ellipticities in degrees deciliter decimeter^{-1} mole^{-1} gauss^{-1};[9]

$$[\theta(a\rightarrow j)]_M = \frac{18N}{\pi N_a^{(0)} H_s}\theta(a\rightarrow j) \tag{1}$$

where N is Avogadro's number, $N_a^{(0)}$, the number of molecules in the unperturbed state, a^0, per unit of volume, and $\theta(a\rightarrow j)$, the observed ellipticity in radians cm^{-1} given by:

$$\theta(a\rightarrow j) = -\frac{4\pi N_a}{\hbar c}\frac{\omega^3\Gamma_{ja}}{(\omega_{ja}^2-\omega^2)^2+\omega^2\Gamma_{ja}^2}Q(a\rightarrow j) \tag{2}$$

$$\begin{aligned}\theta(a\rightarrow j) = Im\{&\langle\Phi_a^0|m_x|\Phi_j^0\rangle\langle\Phi_j^0|m_y|\Phi_a^0\rangle \\ &+ H_s\sum_{k\neq a}(\langle\Phi_k^0|\mu_z|\Phi_a^0\rangle^*\langle\Phi_k^0|m_x|\Phi_j^0\rangle\langle\Phi_j^0|m_y|\Phi_a^0\rangle \\ &+ \langle\Phi_k^0|\mu_z|\Phi_a^0\rangle\langle\Phi_j^0|m_y|\Phi_k^0\rangle\langle\Phi_a^0|m_x|\Phi_j^0\rangle)/\hbar\omega_{ka}^0 \\ &+ H_s\sum_{k\neq j}(\langle\Phi_k^0|\mu_z|\Phi_j^0\rangle^*\langle\Phi_k^0|m_y|\Phi_a^0\rangle\langle\Phi_a^0|m_x|\Phi_j^0\rangle \\ &+ \langle\Phi_k^0|\mu_z|\Phi_j^0\rangle\langle\Phi_a^0|m_x|\Phi_k^0\rangle\langle\Phi_j^0|m_y|\Phi_a^0\rangle)/\hbar\omega_{kj}^0\},\end{aligned} \tag{3}$$

where $\boldsymbol{m}=\sum_i e_i\boldsymbol{r}_i$, $\boldsymbol{\mu}=\sum_i\frac{e_i}{2m_ic}[(\boldsymbol{r}_i\times\boldsymbol{p}_i)+2\boldsymbol{s}_i]$, N_a is the number of molecules in the state, a, per unit of volume in the presence of H_s, and Γ_{ja} is the band width at the half-maximum height of the $a\rightarrow j$ spectral line. The wavefunctions, Φ_a^0, Φ_j^0, and Φ_k^0, are the eigenfunctions of the unperturbed states. If the a^0 and j^0 states are m-fold and n-fold degenerate respectively, the $\theta(a\rightarrow j)$ is given by $\theta(a\rightarrow j)=\sum_{m=1}^{m}\sum_{n=1}^{n}\theta(a_m\rightarrow j_n)$, and the degenerate state wavefunctions are required to diagonalize the magnetic moment, μ_z, in each degenerate state.

For the electronically-allowed transition $a\rightarrow j$ (that is, $\langle\Phi_a|\boldsymbol{m}|\Phi_j\rangle\neq 0$) of a complex with O_h, D_{4h}, and D_{4d} symmetry, the matrix elements, $\langle\Phi_a|\mu|\Phi_j\rangle$ and $\langle\Phi_a|\boldsymbol{\xi}|\Phi_j\rangle$ (where $\boldsymbol{\xi}=\sum_i e_i^2/(4m_ic^2)[\boldsymbol{r}_i(\boldsymbol{r}_i\cdot\boldsymbol{H}_s)-\boldsymbol{H}_s(\boldsymbol{r}_i\cdot\boldsymbol{r}_i)]$), are always equal to zero, because of symmetry properties.

In the present studies of d^8 square-planar metal halides, we choose the Cartesian coordinate system with its origin at the position of the metal atom and with the z-axis perpendicular to the molecular plane. In these complexes, the first term in Eq. (3) is non-zero only when the external magnetic field, $\boldsymbol{H}_s$, is applied in the z-direction. The ground state, a^0, is non-degenerate. Averaging over all the molecular orientations,[9] we obtain:

$$[\theta(a\rightarrow j)]_M = -\frac{720N}{\hbar c}\sum_{n=1}^{n}\frac{\omega^3\Gamma_{j_na}}{(\omega_{j_na}^2-\omega^2)^2+\omega^2\Gamma_{j_na}^2} \times\{Q_A(a\rightarrow j_n)/H_s+Q_B(a\rightarrow j_n)\} \tag{4}$$

where:

7) A. J. McCaffery, P. N. Schatz, and P. J. Stephens, *J. Amer. Chem. Soc.*, **90**, 5730 (1968).
8) P. J. Stephens, *J. Chem. Phys.*, **43**, 4444 (1965).
9) A. D. Buckingham and P. J. Stephens, *Ann. Rev. Phys. Chem.*, **17**, 399 (1966).
10) P. J. Stephens, *J. Chem. Phys.*, **52**, 3489 (1970).
11) L. Rosenfeld, *Z. Physik.*, **57**, 835 (1929).
12) H. A. Kramers, *Proc. Acad. Sci. Amsterdam*, **33**, 959 (1930).
13) R. Serber, *Phys. Rev.*, **41**, 489 (1932).
14) T. Carroll, *Phys. Rev.*, **52**, 822 (1937).
15) M. P. Groenewege, *Mol. Phys.*, **5**, 541 (1962).
16) P. J. Stephens, Theoretical Studies of Magneto-optical Phenomena (Doctoral thesis, Oxford Univ., Oxford 1964).

$$Q_A(a\to j_n) = \frac{1}{3}Im\{\langle\Phi_a^0|m_x|\Phi_{j_n}^0\rangle\langle\Phi_{j_n}^0|m_y|\Phi_a^0\rangle\} \quad (5)$$

and:

$$Q_B(a\to j_n) = \frac{1}{3}Im\{\langle\Phi_a^0|\boldsymbol{m}|\Phi_{j_n}^0\rangle\cdot\sum_{k\neq a}\frac{1}{\hbar\omega_{ka}^0}\langle\Phi_k^0|\boldsymbol{m}|\Phi_{j_n}^0\rangle \times\langle\Phi_k^0|\mu|\Phi_a^0\rangle + \langle\Phi_a^0|m|\Phi_{j_n}^0\rangle \cdot\sum_{k\neq j}\frac{1}{\hbar\omega_{kj_n}^0}\langle\Phi_k^0|\mu|\Phi_{j_n}^0\rangle\times\langle\Phi_k^0|m|\Phi_a^0\rangle\} \quad (6)$$

The wavefunctions for the ground state, a^0, and the excited state, j^0, can be constructed from the normalized anti-symmetrized product functions:

$$\Phi_a^0 = |a\bar{a}b\bar{b}|,\ \Phi_j^0 = \frac{1}{\sqrt{2}}\{|j\bar{a}b\bar{b}| - |\bar{j}ab\bar{b}|\} \quad (7)$$

where a and $\bar{a}$ denote the molecular orbitals, φ_a, with the spin functions of α and β respectively. The excited-state wavefunction, Φ_k^0, must satisfy the conditions; $\langle\Phi_a^0|\boldsymbol{m}|\Phi_k^0\rangle\neq 0$ and $\langle\Phi_k^0|\boldsymbol{\mu}|\Phi_j^0\rangle\neq 0$.

Hence, the wavefunctions must be written as;

$$\Phi_k^0(a\to k) = \frac{1}{\sqrt{2}}\{|k\bar{a}b\bar{b}| - |\bar{k}ab\bar{b}|\}$$

or

$$\Phi_k^0(b\to j) = \frac{1}{\sqrt{2}}\{|a\bar{a}j\bar{b}| - |a\bar{a}\bar{j}b|\} \quad (8)$$

Then, in the molecular orbital form:

$$Q_A(a\to j) = \frac{2}{3}Im\{\langle a|m_x|j\rangle\langle j|m_y|a\rangle\} \quad (9)$$

and:

$$Q_B(a\to j) = \frac{2}{3}Im\left\{\langle a|\boldsymbol{m}|j\rangle\cdot\sum_{k}^{vac}\frac{1}{\hbar\omega_{k(a\to k)a}}\langle k|\boldsymbol{m}|j\rangle\times\langle k|\boldsymbol{\mu}|b\rangle + \langle a|\boldsymbol{m}|j\rangle\cdot\sum_{k\neq j}^{vac}\frac{1}{\hbar\omega_{k(a\to k)j}}\langle k|\boldsymbol{\mu}|j\rangle\times\langle k|\boldsymbol{m}|a\rangle\right\} - \frac{2}{3}Im\left\{\langle a|\boldsymbol{m}|j\rangle\cdot\sum_{b\neq a}^{occ}\frac{1}{\hbar\omega_{k(b\to j)a}}\langle a|\boldsymbol{m}|b\rangle\times\langle j|\boldsymbol{\mu}|b\rangle + \langle a|\boldsymbol{m}|j\rangle\cdot\sum_{b}^{occ}\frac{1}{\hbar\omega_{k(b\to j)j}}\langle a|\boldsymbol{\mu}|b\rangle\times\langle j|\boldsymbol{m}|b\rangle\right\} \quad (10)$$

B. Molecular Orbitals. Yonezawa and his coworkers[17] have proposed a semi-empirical SCF molecular orbital treatment for valence electron systems and have successfully applied it to various small molecules. The present MO calculation is similar to their treatment, but the previous method is improved so as to make it applicable to metal complexes. In the present MO treatment, all valence electrons in a compound are taken into account and all the overlap integrals are considered.

The molecular orbitals, φ's, are expressed as linear combinations of all the valence atomic orbitals, χ_r's, centered on the various atoms of the molecule:

$$\varphi_i = \sum_r C_{ir}\chi_r.$$

We take as χ_r the Slater-type atomic orbital, while the orbital exponents, ζ's, are taken from the tabulations of Clementi.[18] For a closed-shell molecule, the Roothaan SCF equation[19] is written as follows:

$$\sum_r C_{ir}(F_{rs} - S_{rs}\varepsilon) = 0 \quad (s = 1, 2, \cdots) \quad (11)$$

where:

$$F_{rs} = H_{rs} + \sum_{t,u}P_{tu}\{(rs|tu) - 0.5(rt|su)\}, \quad (12)$$

$$S_{rs} = \int\chi_r\chi_s d\tau, \quad (13)$$

$$H_{rs} = \int\chi_r(\mu)H_\mu^{core}\chi_s(\mu)d\tau_\mu, \quad (14)$$

$$(rs|tu) = \int\chi_r(\mu)\chi_s(\mu)\frac{1}{r_{\mu\nu}}\chi_t(\nu)\chi_u(\nu)d\tau_\mu d\tau_\nu, \quad (15)$$

$$P_{tu} = 2\sum_i^{occ}C_{it}C_{iu}. \quad (16)$$

The atomic integrals in the above equations are evaluated by the following approximations. For the electron repulsion integrals, $(rs|tu)$, the Mulliken approximation is adopted;[20]

$$(rs|tu) = 0.25S_{rs}S_{tu}\{(rr|tt) + (rr|uu) + (ss|tt) + (ss|uu)\}.$$

The one-center and two-center Coulomb repulsion integrals are calculated by means of:[21,22]

$$(rr|rr) = I_p^r - E_A^r,\ (rr|ss) = \frac{1}{R+a}$$

where $2/a = (rr|rr) + (ss|ss)$ and where R is the distance between the centers of r and s. The valence-state electron affinity, E_A, is assumed to be equal to the

Table 1. Molecular orbital energies(eV) and orbital characters for $PtCl_4^{2-}$

	Present method	SCCC-MO[a] Basch and Gray	Extended Hückel[b] Cotton and Harris
	$31.44e_u$	$14.8a_{1g}$	8.51
	$21.59a_{1g}$	$11.0e_u$	4.21
	$5.76a_{2u}$; $6p_z$	$-3.6a_{2u}$: $6p_z$	$-4.70a_{2u}$: $6p_z$
L.V.	$1.28b_{1g}$: $5d_{x^2-y^2}$	$-8.0b_{1g}$: $5d_{x^2-y^2}$	$-6.76b_{1g}$: $5d_{x^2-y^2}$
H.O.	$-7.88b_{2g}$: $5d_{xy}$	$-11.5b_{2g}$: $5d_{xy}$	$-10.49b_{2g}$: $5d_{xy}$
	$-7.96e_g$: $5d_{xz,yz}$	$-12.3e_g$: $5d_{xz,yz}$	$-10.68e_g$: $5d_{xz,yz}$
	$-8.02a_{1g}$: $5d_{z^2}$	$-13.3a_{1g}$: $5d_{z^2}$	$-10.98a_{1g}$: $5d_{z^2}$
	$-9.79b_{1g}$	$-13.6b_{2u}$	$-13.49b_{1g}$
	$-9.84e_u$	$-13.6a_{2g}$	$-13.83e_u$
	$-10.00a_{2g}$	$-13.7e_u$	-14.18
	$-10.32b_{2u}$	$-13.7a_{2u}$	-14.58
	$-10.52e_g$	$-14.9e_g$	-14.71
	$-11.35b_{2g}$	$-15.0e_u$	-14.82
	$-11.44a_{2u}$	$-15.2b_{2g}$	-15.09
	$-11.47e_u$	$-16.5a_{1g}$	-15.41
	$-11.77a_{1g}$	$-16.7b_{1g}$	-16.10
	$-18.94b_{1g}$	$-25.4e_u$	-23.29
	$-19.46e_u$	$-25.8b_{1g}$	-23.50
	$-20.06a_{1g}$	$-26.0a_{1g}$	-24.04
Charge on Pt	$=+0.31$	$+0.24$	$+0.44$
Pt–Cl bond order	$=0.489$		0.403

a) Ref. 4, b) Ref. 5.

17) T. Yonezawa, K. Yamaguchi, and H. Kato, This Bulletin **40**, 535 (1967), H. Kato, H. Konishi, and T. Yonezawa, *ibid.*, **40**, 1017 (1967).

18) E. Clementi and D. L. Raimondi, *J. Chem. Phys.*, **38**, 2686 (1963).

19) C. C. J. Roothaan, *Rev. Mod. Phys.*, **32**, 69 (1951).

20) R. S. Mulliken, *J. Chem. Phys.*, **46**, 497, 675 (1949).

21) R. Pariser, *J. Chem. Phys.*, **21**, 568 (1953), R. Pariser and R. G. Parr, *ibid.*, **21**, 767 (1953).

22) N. Mataga and K. Nishimoto, *Z. Physik. Chem. N.F.*, **13**, 140 (1957).

experimental value, and the valence-state ionization potential, I_p, is assumed to be equal to the valence orbital ionization potential (*VOIP*).[23] The values used are given in eV as follows; $(3s3s|3s3s)_{Cl}=9.57$, $(3p3p|3p3p)_{Cl}=11.30$, $(5s5s|5s5s)_{Pd}=7.56$, $(5p5p|5p5p)_{Pd}=3.85$, $(4d4d|4d4d)_{Pd}=8.51$, $(6s6s|6s6s)_{Pt}=8.73$, $(6p6p|6p$-

Table 2a. Molecular orbital for $PtCl_4^{2-}$

MO	Coefficients												
	$6s$	$6p_x$	$6p_y$	$6p_z$	$5d_{xz}$	$5d_{yz}$	$5d_{xy}$	$5d_{x^2-y^2}$	$5d_{z^2}$	$3s^1$	$3p_x^1$	$3p_y^1$	$3p_z^1$
$1a_{1g}$	0.21	0	0	0	0	0	0	0	−0.01	0.44	0.01	0	0
$1e_u$	0	0.14	0	0	0	0	0	0	0	0.65	0.04	0	0
	0	0	0.14	0	0	0	0	0	0	0	0	0.02	0
$1b_{1g}$	0	0	0	0	0	0	0	−0.03	0	0.50	−0.04	0	0
$2a_{1g}$	−0.24	0	0	0	0	0	0	0	0.15	0.12	0.43	0	0
$2e_u$	0	−0.20	0	0	0	0	0	0	0	0.13	0.41	0	0
	0	0	−0.20	0	0	0	0	0	0	0	0	−0.49	0
$1a_{2u}$	0	0	0	0.26	0	0	0	0	0	0	0	0	0.44
$1b_{2g}$	0	0	0	0	0	0	0.21	0	0	0	0	0.47	0
$1e_g$	0	0	0	0	0.22	0	0	0	0	0	0	0	0.69
	0	0	0	0	0	0.22	0	0	0	0	0	0	0
b_{2u}	0	0	0	0	0	0	0	0	0	0	0	0	−0.50
a_{2g}	0	0	0	0	0	0	0	0	0	0	0	−0.51	0
$3e_u$	0	−0.10	0	0	0	0	0	0	0	0.01	0.50	0	0
	0	0	−0.10	0	0	0	0	0	0	0	0	0.50	0
$2b_{1g}$	0	0	0	0	0	0	0	0.29	0	0.03	−0.47	0	0
$3a_{1g}$	−0.15	0	0	0	0	0	0	0	−0.98	0.04	0.07	0	0
$2e_g$	0	0	0	0	−0.98	0	0	0	0	0	0	0	0.18
	0	0	0	0	0	0.98	0	0	0	0	0	0	0
$2b_{2g}$	0	0	0	0	0	0	−0.98	0	0	0	0	0.13	0
$3b_{1g}$	0	0	0	0	0	0	0	0.97	0	−0.07	0.21	0	0
$2a_{2u}$	0	0	0	1.03	0	0	0	0	0	0	0	0	−0.29
$4a_{1g}$	1.27	0	0	0	0	0	0	0	−0.16	−0.40	0.35	0	0
$4e_u$	0	0	1.42	0	0	0	0	0	0	0	0	−0.25	0
	0	−1.42	0	0	0	0	0	0	0	0.67	−0.48	0	0

Table 2b. Molecular orbital and orbital energy(eV) for $PdCl_4^{2-}$

	MO Symmetry	Orbital energy	$5s$	$5p_x$	$5p_y$	$5p_z$	$4d_{xz}$	$4d_{yz}$	$4d_{xy}$	$4d_{x^2-y^2}$	$4d_{z^2}$	$3s^1$	$3p_x^1$	$3p_y^1$	$3p_z^1$
1	$1a_{1g}$	−19.83	0.19	0	0	0	0	0	0	0	−0.01	0.44	0.01	0	0
2	$1e_u$	−19.31	0	0.13	0	0	0	0	0	0	0	0.65	0.04	0	0
3			0	0	0.13	0	0	0	0	0	0	0	0	0.02	0
4	$1b_{1g}$	−18.85	0	0	0	0	0	0	0	−0.02	0	−0.50	−0.04	0	0
5	$2a_{1g}$	−11.64	−0.24	0	0	0	0	0	0	0	0.15	0.12	0.42	0	0
6	$2e_u$	−11.35	0	−0.20	0	0	0	0	0	0	0	0.12	0.41	0	0
7			0	0	−0.20	0	0	0	0	0	0	0	0	−0.48	0
8	$1a_{2u}$	−11.26	0	0	0	0.25	0	0	0	0	0	0	0	0	0.44
9	$1b_{2g}$	−11.20	0	0	0	0	0	0	0.20	0	0	0	0	0.48	0
10	$1e_g$	−10.37	0	0	0	0	0.21	0.01	0	0	0	0	0	0	0.69
11			0	0	0	0	−0.01	0.21	0	0	0	0	0	0	−0.02
12	b_{2u}	−10.18	0	0	0	0	0	0	0	0	0	0	0	0	−0.50
13	a_{2g}	− 9.83	0	0	0	0	0	0	0	0	0	0	0	−0.51	0
14	$3e_u$	− 9.70	0	−0.05	−0.08	0	0	0	0	0	0	0	0.27	0.43	0
15			0	−0.08	0.05	0	0	0	0	0	0	0	0.42	−0.27	0
16	$2b_{1g}$	− 9.46	0	0	0	0	0	0	0	0.26	0	0.04	−0.48	0	0
17	$3a_{1g}$	− 8.39	0.12	0	0	0	0	0	0	0	0.99	−0.03	−0.06	0	0
18	$2e_g$	− 8.36	0	0	0	0	−0.74	0.64	0	0	0	0	0	0	0.13
19			0	0	0	0	0.64	0.74	0	0	0	0	0	0	−0.11
20	$2b_{2g}$	− 8.32	0	0	0	0	0	0	−0.98	0	0	0	0	0.12	0
21	$3b_{1g}$	0.44	0	0	0	0	0	0	0	0.97	0	−0.05	0.19	0	0
22	$2a_{2u}$	5.72	0	0	0	1.03	0	0	0	0	0	0	0	0	−0.28
23	$4a_{1g}$	20.15	1.26	0	0	0	0	0	0	0	−0.12	−0.38	0.34	0	0
24	$4e_u$	28.27	0	−0.21	1.37	0	0	0	0	0	0	0.09	−0.07	−0.24	0
25			0	−1.37	−0.21	0	0	0	0	0	0	0.59	−0.48	0.04	0

23) H. Basch, A. Viste, and H. B. Gray, *J. Chem. Phys.*, **44**, 10 (1966).

Table 3. Calculated excitation energies and transition moments

Transition $i \rightarrow j$	$\delta E(i \rightarrow j)$ (eV)	$\lvert\langle \Psi_i \lvert r \rvert \Psi_j \rangle\rvert^2$ (a_0^2)	$\delta E(i \rightarrow j)$ (eV)	$\lvert\langle \Psi_i \lvert r \rvert \Psi_j \rangle\rvert^2$ (a_0^2)
	$PtCl_4^{2-}$		$PdCl_4^{2-}$	
$^1A_{1g} \rightarrow {}^1E_u$ (1) : $[3e_u - 3b_{1g}]$	7.391	1.166	6.367	0.682
$^1A_{1g} \rightarrow {}^1E_u$ (2) : $[2e_u - 3b_{1g}]$	8.755	0.639	7.794	0.434
$^1A_{1g} \rightarrow {}^1E_u$ $(d-p)$: $[2e_g - 2a_{2u}]$	7.673	0.414	8.357	0.313
$^1A_{1g} \rightarrow {}^1A_{2u}$ (1) : $[b_{2u} - 3b_{1g}]$	7.628	0.010	6.671	0.004
$^1A_{1g} \rightarrow {}^1A_{2u}$ $(d-p)$: $[3a_{1g} - 2a_{2u}]$	7.603	0.757	8.281	0.472

$6p)_{Pt}=4.56$, and $(5d5d|5d5d)_{Pt}=8.60$.

The H_{rr} is given by:

$$H_{rr} = U_{rr} + \sum_{B \neq A} (B|rr) \tag{17}$$

where:

$$U_{rr} = \int \chi_r(\mu) \left\{ -\frac{1}{2} \Delta(\mu) - \frac{Z_A}{r_{\mu A}} \right\} \chi_r(\mu) d\tau_\mu,$$

$$(B|rr) = -\int \chi_r(\mu) \frac{Z_B}{r_{\mu B}} \chi_r(\mu) d\tau_\mu$$

and where Z_A is the number of the valence electrons on the A atom. The molecular integrals, U_{rr} and $(B|rr)$, are approximated by:

$$U_{rr} = -I_r - (N_r - 1)(rr|rr) - \sum_{r' \neq r} N_{r'}(rr|r'r'), \tag{18}$$

$$(B|rr) = -Z_B(s_B s_B|rr), \tag{19}$$

where s_B refers to the valence s-orbital on the B atom.

The $H_{rs(r \neq s)}$ is approximated by:

$$H_{rs} = KS_{rs}(H_{rr} + H_{ss}) \tag{20}$$

where K is a constant taken to be 0.54 in the present calculations.

The molecular orbital energies of $PtCl_4^{2-}$ calculated by the present method are compared with the results of the other MO calculations in Table 1. The lowest vacant (*L.V.*) and the highest occupied (*H.O.*) orbital energies obtained by the present calculation are in good accordance with the values of the electron affinities and the ionization potentials. The obtained d-orbital ordering, $x^2-y^2 > xy > xz, yz > z^2$, is in agreement with the results obtained by others,[4,5] and this ordering is found to be invariant with a variation in the constant K (in Eq. (20)) from 0.53 to 0.56. The orbital energies of the occupied MO's are very close to each other, but this is not serious in the present studies of the MCD of d^8 square-planar complexes. The total charge distribution on Pt is calculated to be +0.310; the details of the electron distribution are $(5d)_{Pt}$; 8.212, $(6s)_{Pt}$: 0.960, $(6p)_{Pt}$: 0.618. The Pt–Cl bond order is calculated to be 0.489.

Calculations were carried out also on $PdCl_4^{2-}$. The MO energies and MO coefficients are presented in Tables 2*a* and 2*b*. The results on $PdCl_4^{2-}$ are nearly equal to those found for $PtCl_4^{2-}$, and the ordering of the MO energies is exactly the same as those of $PtCl_4^{2-}$.

C. Analysis of MCD. As may easily be found from the character table of D_{4h}, the transitions from the ground state, $^1A_{1g}$, to the excited states, $^1A_{2u}$'s or ^1E_u's, are the only allowed transitions. The allowed transitions the calculated excitation energy of which is less than 10 eV are presented in Table 3. The possible allowed transitions, considered previously as the observed high-intensity bands, are all included in the following five transitions: $^1A_{1g} \rightarrow {}^1E_u(1)$: $[3e_u - 3b_{1g}]$, $^1A_{1g} \rightarrow {}^1E_u(d\text{-}p)$: $[2e_g - 2a_{2u}]$, $^1A_{1g} \rightarrow {}^1E_u(2)$: $[2e_u - 3b_{1g}]$, $^1A_{1g} \rightarrow {}^1A_{2u}(1)$: $[b_{2u} - 3b_{1g}]$, and $^1A_{1g} \rightarrow {}^1A_{2u}(d\text{-}p)$: $[3a_{1g} - 2a_{2u}]$. The calculations of Q_A and Q_B by Eq. (9) and (10) were made for these five possible transitions of $PtCl_4^{2-}$; the results are shown in Table 4. The molecular integrals, $\langle k|\boldsymbol{m}|l\rangle$ and $\langle k|\boldsymbol{\mu}|l\rangle$, are accurately evaluated.

Table 4. Calculated values of Q_A and Q_B for each transition in $PtCl_4^{2-}$

Transition	Zeeman energy[a] (cm^{-1})	Q_A $((ea_o)^2)$	Q_B $\left(\frac{(ea_o)^2 \times}{\mu_B/eV}\right)$
$^1A_{1g} \rightarrow {}^1E_u$ (1)	2.669	−0.1943	0.3082
	−2.669	0.1943	0.3082
$^1A_{1g} \rightarrow {}^1E_u$ (2)	2.578	0.1062	−0.1803
	−2.578	−0.1062	−0.1803
$^1A_{1g} \rightarrow {}^1E_u$ $(d\text{-}p)$	2.214	0.0690	−0.8153
	−2.214	−0.0690	−0.8153
$^1A_{1g} \rightarrow {}^1A_{2u}$ (1)	0.0	0.0	−0.3158
$^1A_{1g} \rightarrow {}^1A_{2u}$ $(d\text{-}p)$	0.0	0.0	1.8064

a) Values at H_s=50000 gauss

It should be noted that the molecular integrals, $\langle \chi_A|\boldsymbol{\mu}|\chi_B\rangle$'s, are not Hermitian in some cases if χ_A and χ_B are not atomic orbitals centered on the same atom. In order to eliminate this difficulty, alternative approximate calculations were made. In these approximate calculations, we neglected the $\langle \chi_A|\boldsymbol{\mu}|\chi_B\rangle$ integral if χ_A and χ_B were on different atoms. A comparison of accurately and approximately calculated values of the Zeeman energies and Q_B for each transition in $PtCl_4^{2-}$ is shown in Table 5. The difference between these results is small and is not very important in interpreting the present MCD spectrum.

Table 5. Comparison of exact and approximately calculated values of Zeeman energy and Q_B for each transition in $PtCl_4^{2-}$

Transition	Zeeman energy[a] (cm^{-1})		Q_B $((ea_o)^2\mu_B/eV)$	
	exact	*approx.*	*exact*	*approx.*
$^1A_{1g} \rightarrow {}^1E_u$ (1)	2.669	2.426	0.3082	0.3162
$^1A_{1g} \rightarrow {}^1E_u$ (2)	2.578	3.007	−0.1803	−0.1519
$^1A_{1g} \rightarrow {}^1E_u$ $(d\text{-}p)$	2.214	2.228	−0.8153	−0.8632
$^1A_{1g} \rightarrow {}^1A_{2u}$ (1)	0.0	0.0	−0.3158	−0.1107
$^1A_{1g} \rightarrow {}^1A_{2u}$ $(d\text{-}p)$	0.0	0.0	1.8064	1.6182

a) Values at H_s=50000 gauss

TABLE 6. CALCULATED VALUES Q_A AND Q_B FOR EACH TRANSITION IN $PdCl_4^{2-}$

Transition	Zeeman energy[a] (cm^{-1})	Q_A ($(ea_o)^2$)	Q_A ($(ea_o)^2\times$ / μ_B/eV)
$^1A_{1g}\rightarrow{}^1E_u$ (1)	2.668	−0.1136	0.3923
	−2.668	0.1136	0.3923
$^1A_{1g}\rightarrow E_u$ (2)	2.928	0.0724	−0.2252
	−2.928	−0.0724	−0.2252
$^1A_{1u}\rightarrow{}^1E_u$ (*d-p*)	2.230	0.0521	−0.5824
	−2.230	−0.0521	−0.5824
$^1A_{1g}\rightarrow{}^1A_{2u}$ (1)	0.0	0.0	−0.0301
$^1A_{1g}\rightarrow{}^1A_{2u}$ (*d-p*)	0.0	0.0	1.1102

a) Values at H_s=50000 gauss

Then, we calculated the Zeeman energies and Q_B for each transition in $PdCl_4^{2-}$ by the alternative approximate method described above; the calculated results of Q_A and Q_B are shown in Table 6. The values of the corresponding transitions in $PdCl_4^{2-}$ and $PtCl_4^{2-}$ are very similar to each other. In the above calculations, the effect of spin-orbit coupling is not considered. The atomic constants defined by Condon and Shortley[24] determine the magnitude of the effect. The values of the spin-orbit coupling constant, ζ, for the Cl, Pd, and Pt atoms are listed by McClure[25] as ζ_{3p}^{Cl}=587 cm^{-1}, ζ_{4d}^{Pt}=1410 cm^{-1}, and ζ_{5d}^{Pt}=4060 cm^{-1}. The perturbed ground-state wavefunction is given approximately by:

$$\Phi_{A_{1g}} = \Phi^0_{A_{1g}} - \frac{\langle\Phi^0_{A_{2g}:(2b_{2g}-3b_{1g})}|\zeta^{Pt}_{5d}|\Phi^0_{A_{1g}}\rangle}{\delta E(2b_{2g}-3b_{1g})}\Phi^0_{A_{2g}:(2b_{2g}-3b_{1g})} - \frac{\langle\Phi^0_{E_g:(2e_g-3b_{1g})}|\zeta^{Pt}_{5d}|\Phi^0_{A_{1g}}\rangle}{\delta E(2e_g-3b_{1g})}\Phi^0_{E_g:(2e_g-3b_{1g})} \quad (21)$$

The order of magnitude of the mixing coefficient can be easily estimated; the numerator is, at most, of the order of magnitude of 4000 cm^{-1} ($=\zeta_{5d}^{Pt}$), and the denominator is larger than 20000 cm^{-1}, as may esaily be found from the observed bands. Therefore, the mixing coefficients are smaller than 0.2. Hence, the effect of spin-orbit coupling on the ground-state wavefunction is not significant in the present calculations. The excited-state wavefunctions are also perturbed, but in order to interpret the electronic transition it is not necessary to include this effect in the calculation of high-intensity bands.

Discussion

The theoretical calculations of Q_A and Q_B are necessary in order to interpret the MCD spectrum. The value of Q_A determines whether the observed MCD curve is α-type or β-type; if the value of Q_A for a lower component of the excited state split by the Zeeman energy is positive, then the observed MCD curve is β-type. The values of Q_A and the Zeeman energy can be simply determined by the character of the state wavefunctions; this situation does not depend strongly on the method of the MO calculation. Some of the observed MCD curves for d^8 square-planar metal halides are very similar to each other; this fact suggests that the common assignments hold for these bands. Especially, the higher energy bands of $PdCl_4^{2-}$, $PdBr_4^{2-}$, $AuCl_4^-$, and $AuBr_4^-$ show strongly β-type MCD. Gray and Ballhausen[3c] identified the higher energy band as $^1A_{1g}\rightarrow{}^1E_u(2)$, Jørgensen[1i] suggested the band to be $^1A_{1g}\rightarrow{}^1E_u(2)$, and Basch and Gray[4] later adopted Jørgensen's assignment on the basis of their MO calculation. The results of the numerical calculation for $PdCl_4^{2-}$ shown in Table 6 predict the characteristic types of the MCD curves: the $^1A_{1g}\rightarrow{}^1E_u(1)$ transition is the β-type, the $^1A_{1g}\rightarrow{}^1E_u(2)$ and $^1A_{1g}\rightarrow{}^1E_u(d\text{-}p)$ transitions are both α-type, the $^1A_{1g}\rightarrow{}^1A_{2u}(1)$ transition is γ-type, and the $^1A_{1g}\rightarrow{}^1A_{2u}(d\text{-}p)$ transition is δ-type. The results of the numerical calculation for $PtCl_4^{2-}$ shown in Table 4 also predict the same characterstic types of MCD curves as those of the corresponding transitions for $PdCl_4^{2-}$. We may therefore assign the higher energy bands of $PdCl_4^{2-}$, $PdBr_4^{2-}$, $AuCl_4^-$, and $AuBr_4^-$ to the $^1A_{1g}\rightarrow{}^1E_u(1)$ transitions. We have calculated the line shape of the MCD by taking the center of MCD at the observed value; $\omega_{ja}\simeq$44900 cm^{-1}; the external magnetic field, H_s=50000 gauss, and the band width at half the height of the $a\rightarrow j$ spectral line; Γ_{ja}= 7000 cm^{-1} (*cf.* Fig. 2). The agreement of the calculated MCD curve with the observed one is very good. We may conclude, therefore, that the theory and the experiment are in adequate agreement and the present study of the MCD spectra supports the assignment of the $^1A_{1g}\rightarrow{}^1E_u(1)$ transition. The main feature of the MCD line of shape is determined by Q_A, but the details of the contributions to Q_B from each mixing excited state are interesting; they are shown in Table 7. It should be noted that the magnitude of $Q_B(^1A_{1g}\rightarrow{}^1E_u(1))$ is mainly determined by the contribution from the perturbing excited state: $[2b_{2g}—3b_{1g}]$.

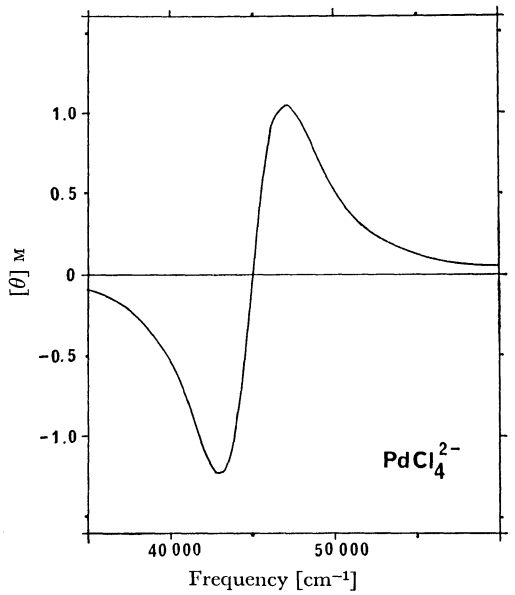

Fig. 2. Computed MCD of $PdCl_4^{2-}$ for $^1A_{1g}$—$^1E_u(1)$ transition

24) E. U. Condon and G. H. Shortley, "The Theory of Atomic Spectra," Cambridge University Press, London and New York 1951, p. 195.

25) D. S. McClure, *J. Chem. Phys.*, **17**, 905 (1949); *Solid State Phys.*, **9**, 399 (1959).

Table 7. Contribution to Q_B $(3e_u-2b_{1g})$ from various excited states in $PdCl_4^{2-}$

Excited state	Contribution to Q_B $((ea_o)^2\mu/eV)$
$[3e_u-4e_u]$	−0.0053
$[1b_{2g}-3b_{1g}]$	−0.0549
$[1e_g-3b_{1g}]$	0.0013
$[2e_g-3b_{1g}]$	0.0323
$[2b_{2g}-3b_{1g}]$	0.4545
$[1e_u-3b_{1g}]$	−0.0084
$[2e_u-3b_{1g}]$	−0.0272
Total	=0.3923

The weaker bands of $AuCl_4^-$ and $AuBr_4^-$ show the γ-type MCD line shape; we consider these bands to be due to only a $^1A_{1g}\rightarrow{}^1A_{2u}(1)$ transition. McCaffery, Schatz, and Stephens[7] suggested that they are composite $^1A_{1g}\rightarrow{}^1A_{2g}+{}^1E_u(1)$ transitions, but the observed intensity of the corresponding absorption band is too small. The present assignments are reasonable in that the magnitude of the calculated transition moment is in accordance with the observed intensity of the absorption band.

Unfortunately, the MCD of the lower energy band at 35800 cm^{-1} of $PdCl_4^{2-}$ has not been reported, but the MCD of $PdBr_4^{2-}$ gives as instructive information on the lower band. The MCD of the band at 30100 cm^{-1} of $PdBr_4^{2-}$ is α-type; it is possibly the $^1A_{1g}\rightarrow{}^1E_u(2)$ or $^1A_{1g}\rightarrow{}^1E_u(d\text{-}p)$ transition. The $^1A_{1g}\rightarrow{}^1E_u(2)$ transition will be on a higher energy side than the $^1A_{1g}\rightarrow{}^1E_u(1)$ transition. It thus seems reasonable to identify it as the $^1A_{1g}\rightarrow{}^1E_u(d\text{-}p)$ transition; this assignment is in agreement with the following assignment of the band at 46200 cm^{-1} in $PtCl_4^{2-}$.

The MCD of the relatively intense band of $PtCl_4^{2-}$ is more complicated than those of paradium halides. Gray and Ballhausen[3c] originally assigned the band to $^1A_{1g}\rightarrow{}^1A_{2u}(1)$, and later Basch and Gray[4] assigned the same band to the two allowed transitions, $^1A_{1g}\rightarrow{}^1A_{2u}(1)$ and $^1A_{1g}\rightarrow{}^1E_u(1)$. The MO calculations on $PtCl_4^{2-}$ by Cotton and Harris[5] predict the band to be the $^1A_{1g}\rightarrow{}^1A_{2u}(d\text{-}p)$ transition. McCaffery, Schatz, and Stephens[7] assigned the shoulder at 43400 cm^{-1} to the $^1A_{1g}\rightarrow{}^1A_{2u}(1)+{}^1E_u(1)$ transition on the basis of the common feature of the shapes of the MCD of this shoulder and on the basis of the lowest energy band in $PdBr_4^{2-}$, while the main band at 46200 cm^{-1} was assigned to the $^1A_{1g}\rightarrow{}^1A_{2u}(d\text{-}p)$ transition by them. However, the quantitative calculation does not support their assignments. The $^1A_{1g}\rightarrow{}^1E_u(1)$ transition is predicted in the above discussion to show strong β-type MCD curves, and the transition is expected to be in a higher energy region, though it is observed in $PdBr_4^{2-}$. The MCD of $PdBr_4^{2-}$ also suggests that the $^1A_{1g}\rightarrow{}^1E_u$ $(d\text{-}p)$ transition will be found among the lower energy bands. We assign the main band at 46200 cm^{-1} to the $^1A_{1g}\rightarrow{}^1E_u(d\text{-}p)$ transition. The $^1A_{1g}\rightarrow{}^1A_{2u}(1)$ transition which is assigned to the lowest energy band in $AuCl_4^-$ and $AuBr_4^-$ will be assigned to the shoulder band at 43400 cm^{-1}. In order to understand the MCD line shape, we should further assign the $^1A_{1g}\rightarrow{}^1A_{1u}(d\text{-}p)$ transitions to the same shoulder band. Taking the center of MCD at the observed point, the external magnetic field $H_s=50000$ cm^{-1}, the width at half the height of a band of the shape $\Gamma_{ja}=5000$ cm^{-1} for the 43400 cm^{-1} band and $\Gamma_{ja}=7000$ cm^{-1} for the 46200 cm^{-1} band, we have calculated the shape of the MCD; the results are shown in Fig. 3. The agreement with the observed MCD line shape is good. The details of the analysis of the contribution to $Q_B(2e_g-2a_{2u})$, $Q_B(b_{2u}-3b_{1g})$, and $Q_B(3a_{1g}-2a_{2u})$ from each mixing

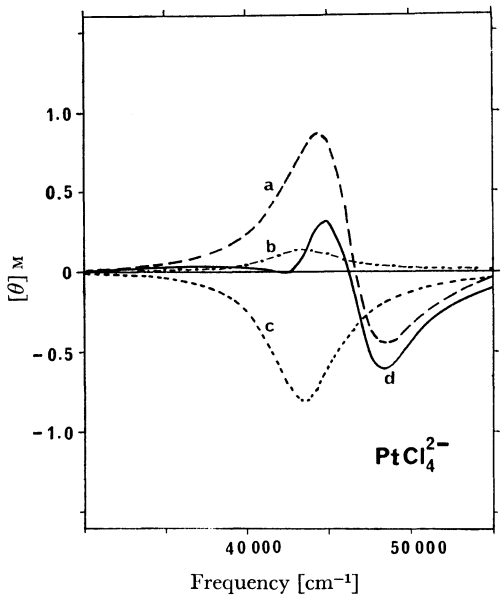

Fig. 3. Computed MCD of $PtCl_4^{2-}$ for $^1A_{1g}$—^1E_u $(d\text{-}p)$ transition: **a**, $^1A_{1g}$—$^1A_{2u}(1)$ transition: **b**, $^1A_{1g}$—$^1A_{2u}$ $(d\text{-}p)$ transition: **c**, and the composite band: **d**.

Table 8. Contribution to Q_B's from various excited states in $PtCl_4^{2-}$ $((ea_o)^2\mu_B/eV)$: unit

Excited state	Contribution to Q_B $(2e_g-2a_{2u})$	Excited state	Contribution to Q_B $(3a_{1g}-2a_{2u})$	Excited state	Contribution ot Q_B $(b_{2u}-3b_{1g})$
$[2e_g-4a_{1g}]$	0.0431	$[3a_{1g}-4e_u]$	0.0014	$[b_{2u}-4e_u]$	−0.0007
$[2e_g-4e_u]$	−0.0021	$[1e_u-2a_{2u}]$	−0.0010	$[1e_g-3b_{1g}]$	−0.2496
$[1e_u-2a_{2u}]$	0.0004	$[2e_u-2a_{2u}]$	−0.0067	$[2e_g-3b_{1g}]$	−0.0416
$[2e_u-2a_{2u}]$	0.0008	$[3e_u-2a_{2u}]$	−0.0100	$[1e_u-3b_{1g}]$	−0.0004
$[3e_{1g}-2a_{2u}]$	0.0007	$[1e_g-2a_{2u}]$	−0.0116	$[2e_u-3b_{1g}]$	−0.0587
$[1a_{1g}-2a_{2u}]$	0.0013	$[2e_g-2a_{2u}]$	1.8343	$[3e_u-3b_{1g}]$	0.0352
$[2a_{1g}-2a_{2u}]$	−0.0097	Total	= 1.8064	Total	= −0.3158
$[1e_g-2a_{2u}]$	−0.0102				
$[3a_{1g}-2a_{2u}]$	−0.8396				
Total	= −0.8153				

TABLE 9. SUMMARY OF THE ASSIGNMENTS

	Observed Transition		Assignment		McCaffery-Schatz[b]-Stephens
	(cm^{-1})	ε_{max}	Present method	Mason-Gray[a]	
$PtCl_4^{2-}$	43400	8500	$^1A_{2u}$ $(d-p)+{}^1A_{2u}$ (1)	$^1A_{2u}$ (1)	$^1A_{2u}$ (1)$+{}^1E_u$ (1)
	46200	10900	^1E_u $(d-p)$	^1E_u (1)	$^1A_{2u}$ $(d-p)$
$PdCl_4^{2-}$	35800	10400		$^1A_{2u}$ (1)$+{}^1E_u$ (1)	$^1A_{2u}$ (1)$+{}^1E_u$ (1)
	44900	28300	^1E_u (1)	^1E_u (2)	^1E_u (2)
$PdBr_4^{2-}$	30100	11500	$^1A_{2u}$ (1)$+{}^1E_u$ $(d-p)$	$^1A_{2u}$ (1)$+{}^1E_u$ (1)	$^1A_{2u}$ (1)$+{}^1E_u$ (1)
	40500	30800	^1E_u (1)	^1E_u (2)	^1E_u (2)
$AuCl_4^-$	32000	5300	$^1A_{2u}$ (1)	$^1A_{2u}$ (1)$+{}^1E_u$ (1)	$^1A_{2u}$ (1)$+{}^1E_u$ (1)
	44500	27500	^1E_u (1)	^1E_u (2)	^1E_u (2)
$AuBr_4^-$	26200	4400	$^1A_{2u}$ (1)	$^1A_{2u}$ (1)$+{}^1E_u$ (1)	$^1A_{2u}$ (1)$+{}^1E_u$ (1)
	39500	36300	^1E_u (1)	^1E_u (2)	^1E_u (2)

a) W. R. Mason and H. B. Gray, *J. Amer. Chem. Soc.*, **90**, 5721 (1968).
b) Ref. 7.

excited state are shown in Table 8. It may be noted that the magnitude of the above Q_B is mainly determined by the contributions from the mixing excited states, $[3a_{1g}-2a_{2u}]$, $[2e_g-2a_{2u}]$, and $[1e_g-3b_{1g}]$ respectively. Especially, we have used the observed values of 43400 cm^{-1} and 46200 cm^{-1} as the excitation energies to the excited states, $[3a_{1g}-2a_{2u}]$ and $[2e_g-2a_{2u}]$ respectively; these are the dominant mixing states.

The present study of the MCD line shape has clarified a number of problems with regard to the assignment of high-intensity bands in d^8 square-planar metal halides. The present assignments are summarized in Table 9, and they are there compared with the previous assignments of others. In some cases, the quantitative calculation is essential; then the MCD becomes the more useful method for understanding the electronic structures of molecules.

The author is grateful to Dr. T. Katô for a very instructive discussion of this article. He also wishes to thank Professor T. Yonezawa and Professor H. Kato for their generous support of this work.